JOURNAL OF MATERIALS SCIENCE: MATERIALS IN MEDICINE 12 (2001) 779–783

Diffuse damage accumulation in the fracture process zone of human cortical bone specimens and its influence on fracture toughness

GAGIK P. PARSAMIAN, TIMOTHY L. NORMAN*
Musculoskeletal Research Center, Departments of Mechanical and Aerospace Engineering and Orthopedics, West Virginia University, Morgantown, WV 26506-9196, USA

This study was concerned with the mechanics and micromechanisms of diffuse (ultrastructural) damage occurrence in human tibial cortical bone specimens subjected to tension–tension fatigue. A nondestructive technique was developed for damage assessment on the surfaces of intact compact tension specimens using laser scanning confocal microscopy. Results indicated that diffuse damage initiates as a result of fractures in the inter-canalicular regions. Subsequent growth of those microscopic flaws demonstrated multiple deflections from their paths due to 3D spatial distribution of microscopic porosities (lacunae–canalicular porosities) and the stress-concentrating effects of lacunae. Damage dominating effects in the early stages of fatigue had been verified by the observed variations of the fracture toughness due to artificially induced amounts of damage. Toughening behavior was observed as a function of diffuse damage.

1. Introduction

Human compact bone has an extremely complex but highly organized microstructure with multiple degrees of hierarchy in its structure [1] and porosity [2]. At the intermediate level of microstructure, the level of opposite extremes of material's structural representation, the key characteristics of the determinants of material properties of compact bone can be realized. Especially, considering the fact that the ''sensors'' of loading alterations in bone, the osteocytes [3], are housed within the lacunae which have an order of size $\approx$ 10–20 μm in diameter.

Understanding of the process of failure of devitalized cortical bone has been a subject of intense research in past few decades. Concepts of linear elastic fracture mechanics (LEFM) have been successfully applied to reveal the mechanics of bone failure including the influence of *in vivo* (e.g. age, sex, etc.) and *in vitro* (e.g. embalming, fixation, etc.) factors [4–13]. The failure of quasi-brittle compact bone [6] is influenced by the development of an intrinsic process zone in the form of a localized region of microcracking. In particular, the process zone has a fundamental importance for defining the structural or system behavior in terms of the post-peak instability, a quantitative size effect and the maximum stress or material strength. Complete understanding of the micro-mechanisms behind the genesis of damage development would ultimately lead to better characterization of bone as a material, better understanding of the pathology of stress fractures and could provide new insights into the mechanisms responsible for the adaptive responses via internal and surface remodeling processes.

Compact tension (CT) fracture toughness specimen geometry has been shown to be appropriate for investigation of the mechanisms of crack nucleation and propagation and its interaction with microstructural features [7]. Vashishth *et al*. [8] demonstrated that bone exhibits a toughening behavior with crack extension and proposed a mechanism of cortical bone fracture with microcracking distribution in the fracture process zone. But the nature of those cumulative processes of damage and its relationship with microstructural architectural configurations of the mineralized tissue is still obscure.

Conventional light microscopy techniques have failed to give an accurate assessment of damage in cortical bone [14, 15]. In particular, fatigue tests have demonstrated that bone exhibits up to 30% stiffness loss prior to the appearance of the first microcracks. Alternative microscopy techniques allowed identification of earlier stages of damage development. Diffuse damage areas, identified as a network of tiny sub-microscopic cracks using back-scattered electron microscopy [16] and laser scanning confocal microscopy (LSCM) [17, 18], have been suggested to be proof of the idea that damage initiates at the ultrastructural level.

The main goal of this study was to monitor damage development in the process zone of CT tibial cortical bone specimens under tensile fatigue loading prior to the

*Author to whom correspondence should be addressed. Department of Orthopedics, Musculoskeletal Research Center, PO Box 9196, Health Science Center, South, West Virginia University, Morgantown, WV 26506-9196.

development of large ($> 50\,\mu m$) cracks. Hence, this study's purpose was to reveal the possible damage initiation sites and the mechanics of damage accumulation. Also, by controlling the amount of induced microflaws in the process zone, investigate the influence of diffuse damage on fracture toughness.

2. Materials and methods

Nineteen CT specimens were machined, under constant water irrigation, from anteromedial, anterolateral and posterior sections of a single cadaver tibia according to procedures outlined elsewhere [10] (Fig. 1a). The tibia was from a 46-year-old male who had died from a cause unrelated to skeletal conditions. All specimens were polished by use of progressively finer grades of sandpaper and finally polished to a mirror finish with Buehler Micropolish 0.1 μm alumina powder. After preparation, all specimens were individually wrapped in 0.9% saline soaked cloth and were kept in airtight containers at $-20\,^{\circ}C$ until testing.

Prior to all tests, specimens were stained with 1% solution of fluorescein sodium salt (Sigma Chem. Co., St. Louis, MO) dissolved in phosphate-buffered isotonic saline (PBS) [19] for histological observations using a Zeiss LSM-510 LSCM system attached to a Zeiss Axioplan 2 fluorescence microscope. To minimize the bleaching problem of the stain associated with laser induced quantum mechanical changes in molecules of the stain, the surfaces of specimens were treated with the *SlowFade-Light* Antifade kit (Molecular Probes, Inc., Eugene, OR). Subsequently specimens were placed on glass slides and were observed for any artifactual cracks and for establishment of baseline *in vivo* diffuse damage. A surface scan of an area ($921.3 \times 921.3\,\mu m^2$) was produced using 10 × objective immediately in front of the crack tip was chosen for damage measurements (Fig. 1b). 20 × and 40 × objectives were subsequently used for subdivision of this area into four sections of $460.6 \times 460.6\,\mu m^2$ and sixteen sections of $230.2 \times 230.2\,\mu m^2$, respectively, for more detailed observations (Fig. 1b).

Diffuse damage areas (Df.Dm.) were identified on the $230.2 \times 230.2\,\mu m^2$ fields and were circumscribed and measured using LSM 510 image processing software. Total Df.Dm. was obtained by summing up the Df.Dm. in all sixteen fields. The diffuse damage density (Df.Dm.D.) parameter was defined as the ratio of total Df.Dm. and bone area (B.Ar)(Df.Dm.D. = Df.Dm./B.Ar., mm^2/mm^2).

After establishing the baseline damage, specimens were submerged in a testing bath filled with Fluorescein stain and cycled in tension at a frequency of 2 Hz on a materials testing system (MTS, Minneapolis, MN) servohydraulic testing machine. Five specimens were randomly chosen from various cortices of the tibia for calibration studies. These studies revealed that 12 N tensile load was an adequate load that was approximately 50% of the typical load necessary to cause deflection from a linear behavior in monotonic loading. Since the purpose of cycling was to induce various amounts of diffuse damage, specimens were not precracked at the chevron notch and the cyclic load induced crack growth was prevented. The amount of artificially induced damage was roughly controlled using the output of the linear variable differential transformer (LVDT) of the MTS machine and by microscopic observations of the surfaces. The residual elongation during cycling was monitored and the cycling was stopped prior to 5–10% loss of specimen stiffness. To monitor the cumulative damage processes, cycling was periodically stopped after every 100–200 cycles and specimens were examined for generated damage using the method described earlier on the LSCM. Cycling was also stopped after the

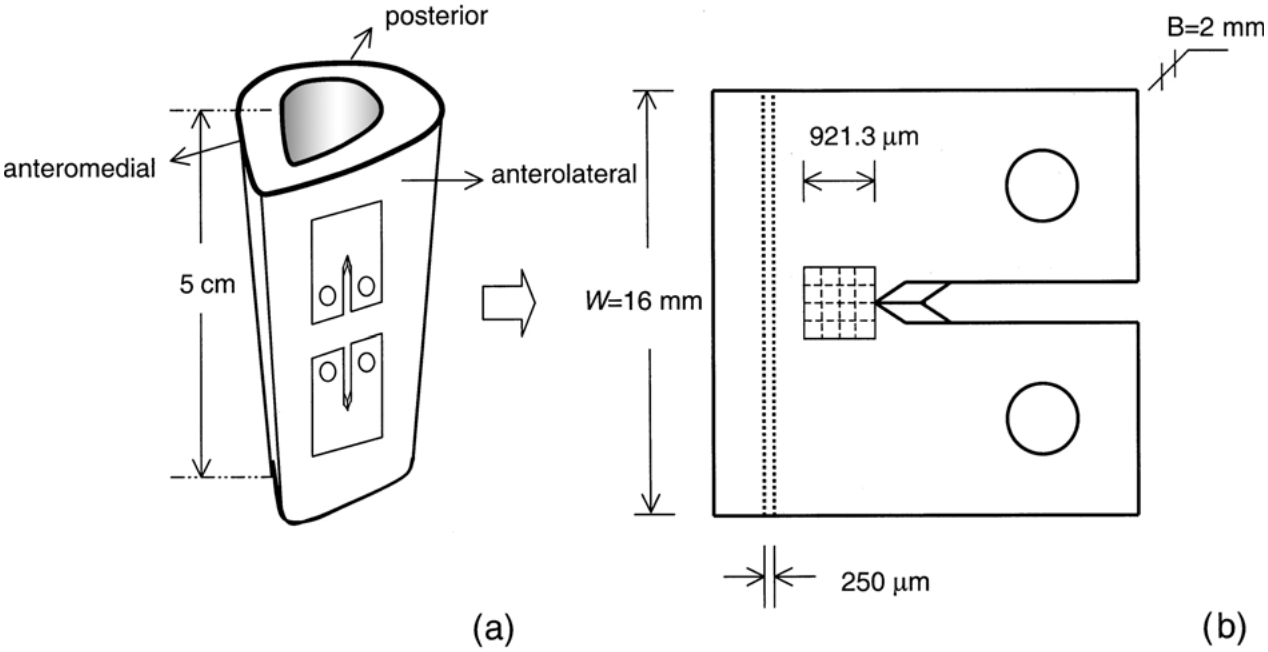

Figure 1 (a) Compact Tension specimens were machined in pairs from anteromedial, anterolateral and posterior cortices of human tibial sections, obtained from distal, medial and proximal locations. (b) Final geometry of specimens with $B = 2$ mm and $a/W = 0.5$. An area of $921.3 \times 921.3\,\mu m^2$ was investigated for damage development. Objectives with higher magnification allowed further subdivision of this area into 4 and 16 fields for more detailed observations. A 250 μm slice, 1 mm away from the chosen area of damage observations, was cut for morphologic analysis of bone microstructure.

appearance of first long ($\approx$ 50–100 μm) microcracks. These measured damage densities served as the ''initial'' damage densities for the subsequent toughness tests.

After achieving adequate amounts of damage in each of the specimens, sharp precracks were introduced with razor blade [10]. Then specimens were submerged back into the testing fixture and were monotonically loaded at a crosshead speed of 2 mm/min [20]. Load and deformation were acquired and the values of stress intensity factors K_{IC} were calculated using Equations (7) and (8) from [7], where $B = 2$ mm and $a/W = 0.5$.

After testing, 250 μm thick stained transverse slices were cut 2 mm ahead of the crack tip (Fig. 1b) of each specimen using a low speed diamond blade metallurgical saw (Buehler, Lake Bluff, IL). Slices were subsequently ground to 150 μm thickness and were polished and mounted on glass slides for morphological analysis using Optimas software under a transmitting light microscope at a power of 40 × [21, 22]. Three adjacent fields, located in the mid section of $2 \times 16\,\text{mm}^2$ cross-sections, were examined and Osteon population density (OsD) and porosity (%P) were measured for all specimens.

Statistical analysis of data was performed using JMP IN® Software (SAS Institute Inc., Cary, NC). Results are reported as mean $\pm$ standard deviation.

3. Results

A nondestructive technique of assessment of damage using intact specimens demonstrated new details of submicroscopic or diffuse damage occurrence. First, histological observations revealed that in the early

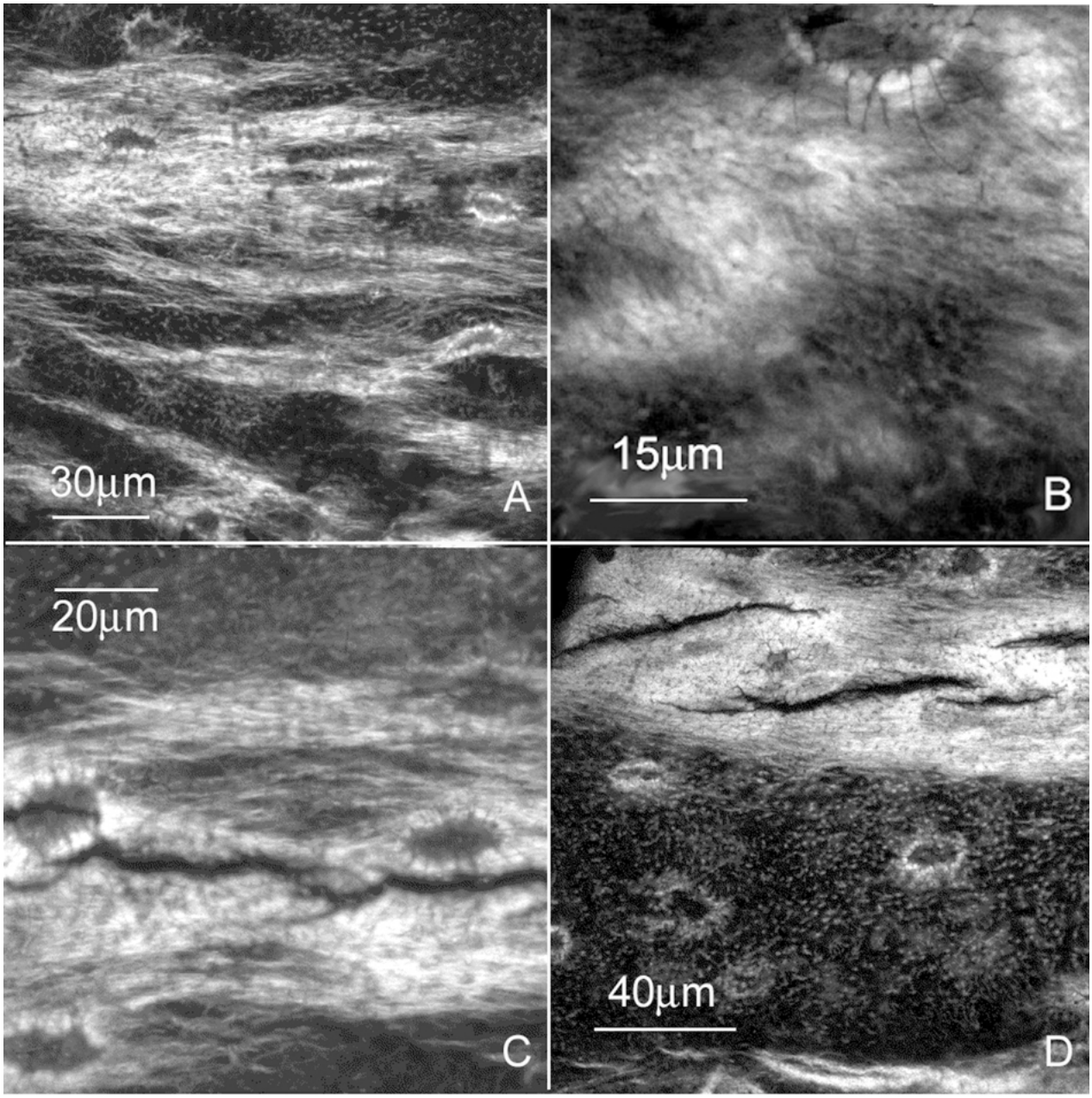

Figure 2 LSCM images of the specimen surfaces (oriented longitudinally to the direction of osteons) with a tensile loading axis perpendicular to the horizontal direction. (A) Typical appearance of diffusely damaged areas demonstrating damaged regions in the canalicular network and lacunae. (B) Pooled region of stain in the intercanalicular space in-between two neighboring lacunae. (C) The path of a crack with multiple deflections passing through a lacuna and passing around another one. This behavior is an indicator of the stress concentrating effects of lacunae. (D) The overlapping nature of microcracking, similar to other engineering materials that experience toughening behavior was observed resulting in long discretized microcracks.

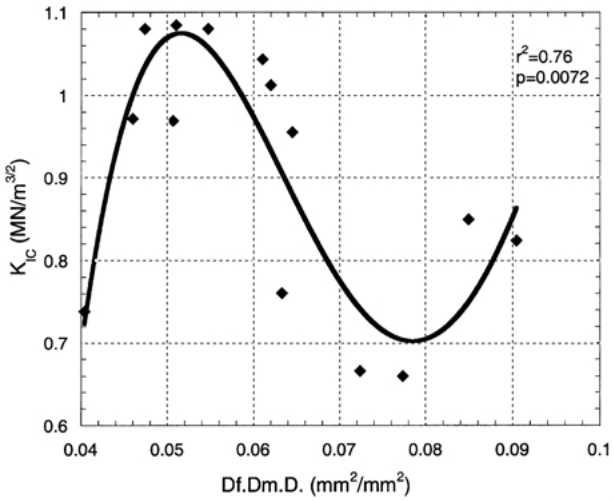

Figure 3 Graph representing the relationship between the fracture toughness (K_{IC}) and diffuse damage (Df.Dm.D).

stages, damaged regions were consistently in the inter-canalicular regions and in the vicinities of lacunae (Fig. 2A). This suggests the possible scenario of damage manifestation as a result of fractures of the mineralized matrix in the inter-canalicular regions. The vacuum regions generated by the process of fracture cause a stain uptake resulting in pooled regions of stain in the vicinities of lacunae (Fig. 2B). Excitation of the Fluorescein molecules reveals the location of damage. The thickness of intact specimens did not allow us to use higher magnification objectives and we were not able to visualize sharp boundaries of the ultra-structural cracks. Therefore, at this level, damaged areas appear blurry and pooled (Fig. 2B). As the defects grew larger, on the order of the lacunae, the boundaries were more evident and the cracks became distinct microscopic cracks (Fig. 2C and D).

Cyclic loading caused an increase in diffuse damage with a corresponding decrease of 5–10% in the initial stiffness (198.23 ± 27.35 N/mm). Critical loads, P_C, obtained from the load-deflection data, were used to calculate the corresponding stress intensity factors (K_{IC}) that were plotted against Df.Dm.D (Fig. 3). Fourth degree polynomial fitting was chosen for the nonlinear regression analysis of the data. Statistical analysis showed significant correlation between fracture toughness and diffuse damage ($r^2 = 0.76$, $p = 0.0072$).

Analysis of variance (ANOVA) demonstrated no statistically significant variation of morphological parameters ($\mathrm{OsD} = 14.3643 \pm 1.9524$, $\#/\mathrm{mm}^2$; $\%\mathrm{P} = 7.3878 \pm 1.29$, $\mathrm{mm}^2/\mathrm{mm}^2$) with either bone location (distal, medial, proximal) ($r^2 = 0.07$, $p = 0.66$; $r^2 = 0.31$, $p = 0.14$) or cortex location (anteromedial, anterolateral, posterior) ($r^2 = 0.041$, $p = 0.79$; $r^2 = 0.04$, $p = 0.78$).

4. Discussion

The characteristic time of all kinetic processes in solids, including phase transformation and breaking of bonds between the elements of microstructure, decreases very strongly with growing tensile stresses [23]. Therefore, at the tips of cracks where there is a strong stress concentration, fracture processes are usually complicated by microstructural transformations, heat generation and microscopic damage accumulation. The damage process zone (DPZ) is referred to as the zone where interactions take place between microscopic flaws in the process of microcrack growth giving rise to strain localization within this narrow band. According to continuum mechanics, within this zone the bearing capacity is reduced as a consequence of an inelastic increment in strain thus leading to the phenomenon that violates Drucker's stability postulate [24] making classical theory of plasticity inapplicable [25].

Our observations suggest that diffuse damage in cortical bone is a result of breakdowns in the canalicular network (Fig. 2A). The fractures of hydroxyapatite crystals surrounding collagen fibers or delaminations at the crystal–fiber interfaces could provide a possible explanation of the onset of these damaging processes. Structural delaminations as a result of the damaging events generate micro-vacuum regions, which subsequently cause a stain uptake. Those delaminations are very small; therefore, those newborn regions appear blurry and pooled (Fig. 2B). Growth of those defects tends to open up lacunae in a direction perpendicular to the local stresses. It was interesting to observe that spatial distribution of lacunae and the canalicular network interconnecting those lacunae often caused cracks to deflect from their paths upon meeting with lacunae (Fig. 2C) thus leading to the formation of discretized microcracks (Fig. 2D). Overall histological observations could be summarized into the following possible micromechanism of damage evolution: damage onset, as a result of fractures in crystals within the intra-canalicular matrix; subsequent growth into intra-canalicular cracks, as a result of possible delaminations between collagen bundles; and multiple deflections of those cracks, due to three-dimensional distribution of canaliculi and lacunae and the stress concentrating effects of lacunae.

Results from fracture toughness tests demonstrated that sub-microscopic damaging events are the mechanisms behind the stiffness degradations in early stages of fatigue proposed in the studies by Burr *et al*. [14] and Schaffler *et al*. [15]. Results indicated that bone exhibits a toughening behavior as a function of diffuse damage (Fig. 3). The explanation for this behavior lies within the frontal damage zone formed around the crack tip and the energy consumption processes within this zone [26–30]. Strain energy associated with the formation of flaws, as a result of damaging events, serves as the toughening increment. The first rising phase in Fig. 3 indicates that, as diffuse damage accumulates, bone toughens until it reaches some ''threshold'' value of damage when microcracks first start to appear resulting in a decrease of toughness (falling phase of the graph in Fig. 3). Then, more diffuse damaging processes and the interactions of those microflaws cause an increase in toughness again (second rising phase in Fig. 3). This phenomenon could be a part of the behavior that toughness experiences as a function of the number of microcracks. But since the goal of this study was to investigate bone's response to diffuse damage accumulation and the damaging loading was stopped prior to the appearance of major cracks, the relationship between toughness and the number of cracks

was not investigated. Vashishth *et al*. [8] demonstrated the toughening behavior associated with macrocrack extension and the increase in the number of microcracks. This toughening behavior at the ultra-structural level could provide an adequate ''time'' for a biological response prior to the growth of those sub-microscopic flaws and the subsequent catastrophic irreversible effects in the material's behavior. It was also interesting to observe that the threshold values of Df.Dm.D were $\approx 5\%$, which was very close to the amount of *in vivo*, diffuse damage ($\approx 3\%$) [31] supporting the idea that damage serves as a constant maintenance stimulus of bone [32–34].

It is important to outline the limitations of this study. All specimens were obtained from a single bone, leaving the question of the donor variability of this study unanswered. Also, we considered only one of the many possible loading regimens to which long bones are subjected throughout their lives. Nevertheless, this study demonstrated new insights into the early stages of damaging processes in bone and proved that confocal microscopy is a good technique for nondestructive evaluation of damage morphology in bone.

Acknowledgments

The authors would like to thank Vincent Kish for assistance with the mechanical tests and Dr Peter Zioupos from Cranfield University, UK, for providing the details of the staining protocol. This work was supported by the National Institutes of Health (NIH) – National Institute of Aging (R01 AG 14682-01A1).

References

1. R. LAKES, *Nature* **361** (1993) 511.
2. S. C. COWIN, *J. Biomech.* **32** (1999) 217.
3. L. E. LANYON, *Calcif. Tissue Intl.* **53**(Suppl. 1) (1993) S102.
4. T. M. WRIGHT and W. C. HAYES, *J. Biomech.* **10** (1977) 419.
5. W. BONFIELD and P. K. DATTA, *ibid.* **9** (1976) 131.
6. J. C. BEHIRI and W. BONFIELD, *ibid.* **17** (1984) 25.
7. W. BONFIELD, *ibid.* **20** (1987) 1071.
8. D. VASHISHTH, J. C. BEHIRI and W. BONFIELD, *ibid.* **30** (1997) 763.
9. T. L. NORMAN, D. VASHISHTH and D. B. BURR, *ibid.* **28** (1995) 309.
10. T. L. NORMAN, S. V. NAVARGIKAR and D. B. BURR, *ibid.* **29** (1996) 1023.
11. Y. N. YENI, C. U. BROWN and T. L. NORMAN, *Bone* **22** (1998) 71.
12. T. L. NORMAN, Y. N. YENI, C. U. BROWN and Z. WANG, *ibid.* **23** (1998) 303.
13. P. ZIOUPOS and J. D. CURREY, *ibid.* **22** (1998) 57.
14. D. B. BURR, C. H. TURNER, P. NAICK, M. R. FORWOOD, W. AMBROSIUS, M. S. HASSAN and R. PIDAPARTI, *J. Biomech.* **31** (1998) 337.
15. M. B. SCHAFFLER, T. M. BOYCE and D. P. FYHRIE, *Transactions of the 42nd Annual Meeting, Orthopedic Research Society* **21** (1996) 57.
16. M. B. SCHAFFLER, W. C. PITCHFORD, K. CHOI and J. M. RIDDLE, *Bone* **15** (1994) 483.
17. P. ZIOUPOS and J. D. CURREY, *J. Mater. Sci.* **29** (1994) 978.
18. T. M. BOYCE, D. P. FYHRIE, M. C. GLOTKOWSKI, E. L. RADIN and M. B. SCHAFFLER, *J. Orth. Res.* **16** (1998) 322.
19. P. ZIOUPOS, X. T. WANG and J. D. CURREY, *Clin. Orthop.* **11** (1996) 365.
20. ASTM Standards E399-83 Standard Test Method for Plane-Strain Fracture Toughness of Metallic Materials. American Society for Testing and Materials, Philadelphia, PA, 1985: 03.01.
21. R. B. MARTIN and J. ISHIDA, *J. Biomech.* **22** (1989) 419.
22. R. W. BARTH, C. B. RUFF and K. BISSESSUR, *Clin. Ortho. Rel. Res.* **283** (1992) 178.
23. G. I. BARENBLATT and L. R. BOTVINA, *Bull. Acad. Sci. USSR*, **4** (1983) 88.
24. D. C. DRUCKER, *Appl. Mech. Rev.* **41** (1988) 151.
25. Z. P. BAZANT, *ibid.* **39** (1986) 675.
26. P. F. BECHER, *J. Amer. Ceram. Soc.* **74** (1991) 255.
27. B. BUDIANSKY, J. W. HUTCHINSON and J. C. LAMBROPOULUS, *Int. J. Solids Structs.* **19** (1983) 337.
28. K. T. FABER and A. G. EVANS, *Acta. Metall.* **31** (1983) 565.
29. K. T. FABER and A. G. EVANS, *ibid.* **31** (1983) 577.
30. Y-W. MAI, *Mater. Forum.* **11** (1988) 289.
31. T. L. NORMAN, G. P. PARSAMIAN and C. B. COLEMAN, *Transactions of the 47th Annual Meeting, Orthopaedic Research Society* **26** (2001) 15.
32. R. B. MARTIN and D. B. BURR, in ''The Structure, Function and Adaptation of Cortical Bone'' (Raven Press, New York, 1989).
33. H. M. FROST, in ''Bone remodeling and its relationship to metabolic bone diseases'' (Charles C. Thomas, Springfield, IL, 1973).
34. D. R. CARTER, D. P. FYHRIE and R. T. WHALEN, *J. Biomech.* **20** (1987) 785.

Received 12 June
and accepted 28 July 2000